

This work was written as part of one of the author's official duties as an Employee of the United States Government and is therefore a work of the United States Government. In accordance with 17 U.S.C. 105, no copyright protection is available for such works under U.S. Law.

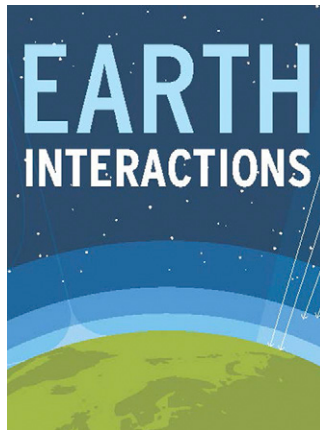
Public Domain Mark 1.0

<https://creativecommons.org/publicdomain/mark/1.0/>

Access to this work was provided by the University of Maryland, Baltimore County (UMBC) ScholarWorks@UMBC digital repository on the Maryland Shared Open Access (MD-SOAR) platform.

Please provide feedback

Please support the ScholarWorks@UMBC repository by emailing scholarworks-group@umbc.edu and telling us what having access to this work means to you and why it's important to you. Thank you.



Copyright © 2017, Paper 21-003; 20656 words, 4 Figures, 0 Animations, 2 Tables.
<http://EarthInteractions.org>

Approximating Long-Term Statistics Early in the Global Precipitation Measurement Era

Thomas Stanley

Universities Space Research Association, and Goddard Earth Sciences Technology and Research, Columbia, and Hydrological Sciences Laboratory, NASA Goddard Space Flight Center, Greenbelt, Maryland

Dalia B. Kirschbaum^a

Hydrological Sciences Laboratory, NASA Goddard Space Flight Center, Greenbelt, Maryland

George J. Huffman

Mesoscale Atmospheric Processes Laboratory, NASA Goddard Space Flight Center, Greenbelt, Maryland

Robert F. Adler

Earth System Sciences Interdisciplinary Center, University of Maryland, College Park, College Park, Maryland

Received 23 August 2016; in final form 6 February 2017

^a Corresponding author e-mail: Dalia B. Kirschbaum, dalia.b.kirschbaum@nasa.gov

ABSTRACT: Long-term precipitation records are vital to many applications, especially the study of extreme events. The Tropical Rainfall Measuring Mission (TRMM) has served this need, but TRMM's successor mission, Global Precipitation Measurement (GPM), does not yet provide a long-term record. Quantile mapping, the conversion of values across paired empirical distributions, offers a simple, established means to approximate such long-term statistics but only within appropriately defined domains. This method was applied to a case study in Central America, demonstrating that quantile mapping between TRMM and GPM data maintains the performance of a real-time landslide model. Use of quantile mapping could bring the benefits of the latest satellite-based precipitation dataset to existing user communities, such as those for hazard assessment, crop forecasting, numerical weather prediction, and disease tracking.

KEYWORDS: Central America; Satellite observations; Statistical techniques; Model evaluation/performance; Model output statistics

1. Introduction

Many users of precipitation data require long-term records, especially when characterizing extreme events. Satellite-based precipitation estimates can meet this need in locations without dense gauge networks. The National Aeronautics and Space Administration (NASA) has been providing near-real-time precipitation data to the community since 2002 (Huffman et al. 2010, 2007). The Tropical Rainfall Measuring Mission (TRMM) was launched in November 1997. Its successor, the Global Precipitation Measurement (GPM) *Core Observatory*, was launched in February 2014 and extends observations of both falling snow and heavy to light rain past 65°N/S (Hou et al. 2014). To provide nearly global coverage with short revisit times, the TRMM and GPM missions rely on a constellation of partner satellites. The TRMM Multisatellite Precipitation Analysis (TMPA) covers the area from 50°N/S from 2000 to present (Table 1), while the Integrated Multisatellite Retrievals for GPM (IMERG) covers 60°N/S from March 2014 to the present (Huffman et al. 2015).

Because of the use of different sensors, algorithms, and calibrations, the IMERG and TMPA products differ considerably. A comparison of percentiles from 7 March 2015 to 6 March 2016 for the GIS-formatted IMERG Version 3 Late Run (IMERG-L) and Real-Time TMPA, version 7 (TMPA-RT), daily products (Huffman 2016a,b) revealed some of the characteristics of these differences (Figure 1). Days with zero estimated precipitation were included in the distribution because TMPA-RT and IMERG-L differ in the ability to detect very light precipitation (Hou et al. 2014). At specific percentiles, the TMPA-RT values were resampled to a 0.1° grid by the nearest neighbor method, and then the IMERG-L values were subtracted. At the 75th percentile (Figure 1a), there are small differences between TMPA-RT and IMERG-L, but differences of more than 100 mm day⁻¹ occur at the 95th percentile (Figure 1b). TMPA-RT tends to show heavier tropical precipitation (blue), and IMERG-L tends to show heavier midlatitude precipitation (red). In particular, the Southern Ocean shows a large and relatively consistent difference between IMERG-L and TMPA-RT. However, many locations do not fit this pattern, including some mountainous regions and inland water bodies. In addition to geographic heterogeneity, the relationship between TMPA-RT and IMERG-L may vary seasonally and interannually. Combined, these factors complicate the use of IMERG data in TMPA-based applications.

Table 1. Summary of TRMM and GPM multisatellite products, resolutions, availability, and latency. The TRMM level-3 multisatellite product TMPA has a near-real-time version that is calibrated with a gauge climatology and a research product that uses a global network of gauges to calibrate the product. GPM level-3 IMERG has three versions: the early run is produced with a latency of 4–5 h after satellite acquisition, the late run uses more satellite information and an improved morphing scheme, and a final run uses a global gauge network to calibrate the observations.

Satellite	Algorithm name	Resolution		Coverage	Available	Latency
		Space	Time			
TRMM	TMPA version 7	$0.25^{\circ} \times 0.25^{\circ}$	3 h	Gridded, 50°N–50°S	2000–present	8 h (real time)
					1998–present	2 months (research)
GPM	IMERG	$0.1^{\circ} \times 0.1^{\circ}$	30 min	Gridded, 65°N–65°S	April 2015–present	4–5 h (early run)
					March 2015–present	14–15 h (late run)
					March 2014–present	3 months (final run)

Satellite precipitation data are used in many applications such as flood monitoring, crop forecasting, numerical weather prediction, and disease tracking (Kucera et al. 2013; Kirschbaum et al. 2017). These user communities have relied upon TMPA data, and several workshops have highlighted the need for long precipitation records (Ward et al. 2015; Ward and Kirschbaum 2014). While the GPM mission plans to create a consistent record of precipitation available from 1998 to the present using TRMM, GPM, and partner data, this processing is not planned to begin before 2018. Until that happens, application developers could take advantage of IMERG’s improved spatial and temporal resolution and accuracy while maintaining the benefits of TMPA’s long time series by adapting IMERG data to TMPA-equivalent values with quantile mapping. Quantile mapping [also known as quantile matching, cumulative distribution function (CDF) matching, etc.] has been used to convert gridded precipitation data to its point-based equivalent (Gudmundsson et al. 2012), to adapt gridded precipitation data to a different spatial resolution (Maraun 2013), and to correct model bias at the same resolution as observational data (Cannon et al. 2015). Gudmundsson et al. (2012) recommended the use of nonparametric data transformations (e.g., empirical quantiles) for reducing biases across the entire distribution, so these methods may be more appropriate for transforming extreme values such as rainfall thresholds. An example of the statistical transformation of an empirical rainfall distribution can be found in the second chapter of Panofsky and Brier (1958).

To demonstrate the use of IMERG in a TMPA-based application, quantile mapping from TMPA-RT to IMERG-L was applied to the Landslide Hazard Assessment for Situational Awareness (LHASA) model. LHASA issues a daily nowcast with a resolution of approximately 1 km (Kirschbaum et al. 2015a). The nowcast includes both a moderate hazard level to maximize sensitivity and a high hazard level to reduce the number of false alarms. LHASA combines rainfall and landslide susceptibility with a heuristic decision tree in three stages: first, areas rated “very low” on the landslide susceptibility map of Central America and the Caribbean Islands (Kirschbaum et al. 2015b) are excluded from further analysis; second, a 60-day antecedent rainfall index is calculated from TMPA-RT; and third,

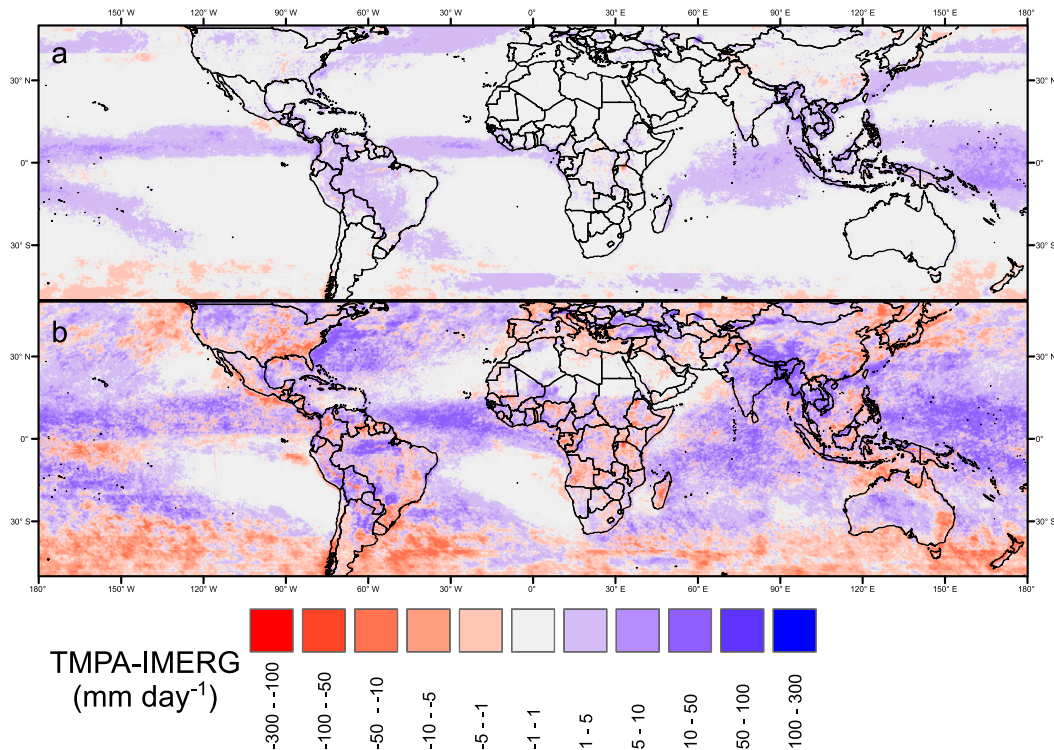


Figure 1. Difference between TMPA-RT (regridged to 0.1°) and IMERG-L from 7 Mar 2015 to 6 Mar 2016 for the daily (a) 75th and (b) 95th percentiles. Positive values indicate areas where TMPA-RT is higher (blue), and negative areas show that IMERG-L is higher (red). At these percentiles, no difference was observed in many arid regions, but differences can be observed in those regions during rare precipitation events.

the current daily rainfall accumulation is compared to one of two climatological thresholds, depending upon the level of antecedent rainfall. LHASA was calibrated over the period 2007–13 with reference to the global landslide catalog (GLC), an inventory of rainfall-triggered landslides reported by media and other sources (Kirschbaum et al. 2015c, 2010). LHASA was validated by the GLC events occurring in 2014.

2. Methods

LHASA was developed and calibrated with TMPA-RT precipitation estimates, but the transition from TRMM to GPM required that the model be updated to use IMERG-L inputs, which do not currently have the long record needed for development of the necessary rainfall–landslide relations. The quantile mapping technique was accomplished in four main steps: 1) evaluation of data time series and characteristics, 2) selection of space–time domain, 3) quantile calculations, and 4) quantile mapping through LHASA case study. Nearly 17 years of TMPA-RT and 1.2 years of IMERG-L were available for this case study.

First, the characteristics of each dataset were considered. Both products are produced at a moderate spatial resolution, but the finer resolution of IMERG-L is associated with higher precipitation estimates for extreme events, as expected. Land and sea pixels exhibit distinct rainfall patterns in both IMERG-L and TMPA-RT. The relationship between products is spatially heterogeneous on land (Figure 1), is not controlled solely by elevation, and is likely to be difficult to predict on the basis of other variables.

Second, the selection of a space–time domain on which to perform quantile mapping represents a compromise between sample size and the relevance of the empirical distributions to a specific time and place (Reichle and Koster 2004; Voisin et al. 2010). The short time period for which IMERG-L is available, combined with the relatively homogeneous time series, suggested that calculation of separate monthly quantiles would reduce the sample size, without making the data transformation much more representative of each month. Therefore, all data from 6 May 2015 to 5 May 2016 were assigned to the same domain. Spatial heterogeneity of precipitation estimates across the region implied that it would be beneficial to partition the data before quantile mapping, but the absence of strong ties between the difference maps and elevation, land cover, or standard climate zones made it difficult to do so on an a priori basis. More importantly, LHASA focuses on extreme rainfall events. This upper tail of the distribution is best described by a large sample. Therefore, the entire land area was assigned to a single domain. Marine pixels were not included because these are not representative of rainfall on land.

Third, 100 000 quantiles were calculated for the TMPA-RT and IMERG-L products in the statistical software R (R Core Team 2015; Hijmans 2015). The large number of quantiles (1 cut point for every 0.001% of each distribution) approximated the empirical CDF and minimized the error associated with interpolation of extreme rainfall. Then the quantiles for IMERG-L and TMPA-RT were paired into a single table that described the whole land area over 1 year. Fourth, the table was applied to each LHASA daily rainfall threshold (based on TMPA-RT) to produce equivalent IMERG-L thresholds (Figure 2). These four steps were repeated for values of the 60-day antecedent rainfall index.

Fourth, the quantile-mapped version of LHASA was run with IMERG-L data. The performance of the adapted rainfall thresholds was evaluated by a comparison to the original TMPA-based model. The true positive rate (TPR) was determined by calculating the proportion of reported landslide events (GLC) that were predicted correctly by LHASA. There may be some error in the reported dates of GLC events (Kirschbaum et al. 2015c). To address this issue, TPR was calculated for 1-, 3-, and 7-day windows (e.g., if LHASA correctly predicted a landslide that occurred 2 days before its reported date, it would be counted as a true positive only for the 7-day window). The number of pixel days for which a nowcast was issued without a GLC event was divided by the total number of pixel days to determine the false positive rate (FPR). These results were also compared to the LHASA calibration period.

3. Results

In general, the version of LHASA with IMERG-adapted thresholds remained very similar to the TMPA version. Figure 3 shows the TMPA rainfall thresholds (Figure 3a) and the new IMERG thresholds (Figure 3b). The magnitude of the

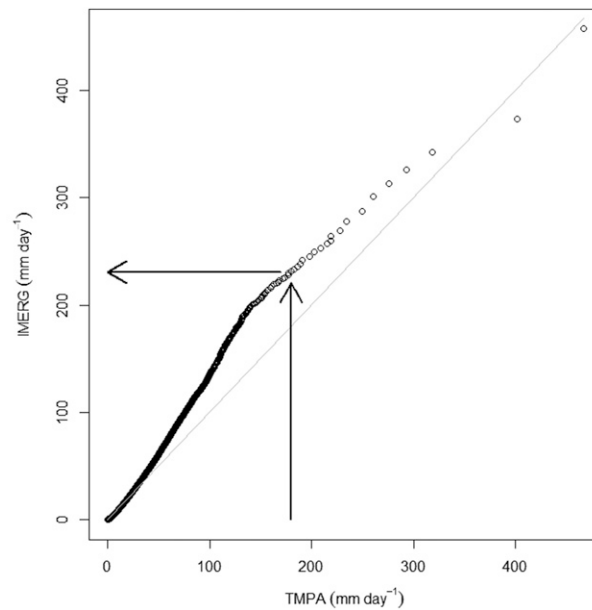


Figure 2. Quantile–quantile plot for the Central American land area for 6 May 2015–5 May 2015. 100 000 quantiles (open circles) were calculated for the TMPA-RT and IMERG-L rainfall estimates. In quantile mapping, a value from one product is used to look up the value of the second product at the same quantile. For example, if a TMPA-RT precipitation threshold was 180 mm day^{-1} , the equivalent IMERG-L value would be 231 mm day^{-1} .

change was greatest in the wettest locations due to differences in calibration, the shift to finer resolution, or both. Model performance with IMERG-L was comparable to TMPA-RT for both the high hazard and moderate hazard nowcasts (Table 2). The FPR was consistent across inputs because quantile mapping maintains the frequency with which a threshold will be exceeded. Although better results were obtained during the model calibration period (2007–13), TMPA-RT and IMERG-L produced comparable postcalibration performance.

Although the overall performance was good (Table 2), the high hazard model run with IMERG-L produced a FPR over 20% in San José, Costa Rica. The anomaly did not occur elsewhere and was caused by the fact that the IMERG record shows unusually frequent and heavy rainfall in the Costa Rican capital (Figure 4) compared to the nearby site of El Bosque as well as the entire region. Thus, the single Central American domain was not representative of the relationship between IMERG and TMPA at this site, and quantile mapping did not correct the local bias.

4. Discussion

LHASA showed comparable performance for IMERG and TMPA inputs, which suggests that quantile mapping successfully adapted the model to the new precipitation data stream. It is anticipated that subsequent versions of IMERG will

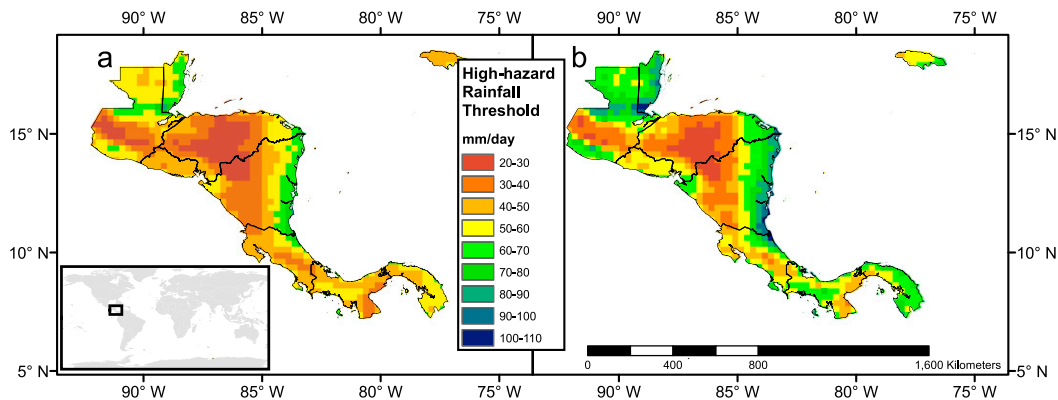


Figure 3. (a) The LHASA high hazard rainfall threshold was calculated from TMPA-RT data for the period 2001–14. (b) The quantile-mapped IMERG-L equivalent thresholds.

further improve the precipitation estimates, particularly for extreme rainfall. However, performance varied locally. Anomalous locations may be poorly served by quantile mapping across a single time–space domain. If the application was focused on such a location, quantile mapping should be applied more locally.

In other study areas and for other applications, it may be appropriate to use a different quantile mapping scheme. In cases where a large amount of data is available and the relationship between TMPA and IMERG varies seasonally, it may be helpful to segment the data by month or season before quantile mapping (e.g., [Turkington et al. 2016](#); [Wood et al. 2004](#)). In cases with little to no seasonal variation, it may be appropriate to include partial years in the precipitation distribution. The land surface could be divided into elevation or climate zones, if these features were consistently associated with biases in the precipitation data. In cases

Table 2. The performance of TMPA-RT and IMERG-L was compared by determining the number of landslides predicted by each model run. This table shows (a) precipitation product; (b) corresponding date range; (c) version of LHASA that was tested; (d) number of landslides reported during each time period; (e)–(g) proportion of landslides for which a nowcast was issued on the reported date (1 day), the day before or after the reported event (3 day), and within a 7-day window around the reported date, respectively; and (h) FPR or overall frequency with which LHASA issues nowcasts at dates and places without recorded landslides.

(a) Model input	(b) Date range of model run	(c) Hazard level	(d) Landslide reports	(e) 1-day TPR	(f) 3-day TPR	(g) 7-day TPR	(h) FPR
TMPA-RT	2007–13	Moderate	99	64%	77%	83%	11%
TMPA-RT	2014	Moderate	43	58%	74%	79%	9%
TMPA-RT	May 2015–May 2016	Moderate	73	45%	73%	84%	6%
IMERG-L	May 2015–May 2016	Moderate	73	56%	73%	82%	10%
TMPA-RT	2007–13	High	99	26%	37%	47%	1%
TMPA-RT	2014	High	43	12%	33%	47%	1%
TMPA-RT	May 2015–May 2016	High	73	15%	29%	37%	1%
IMERG-L	May 2015–May 2016	High	73	12%	40%	49%	1%

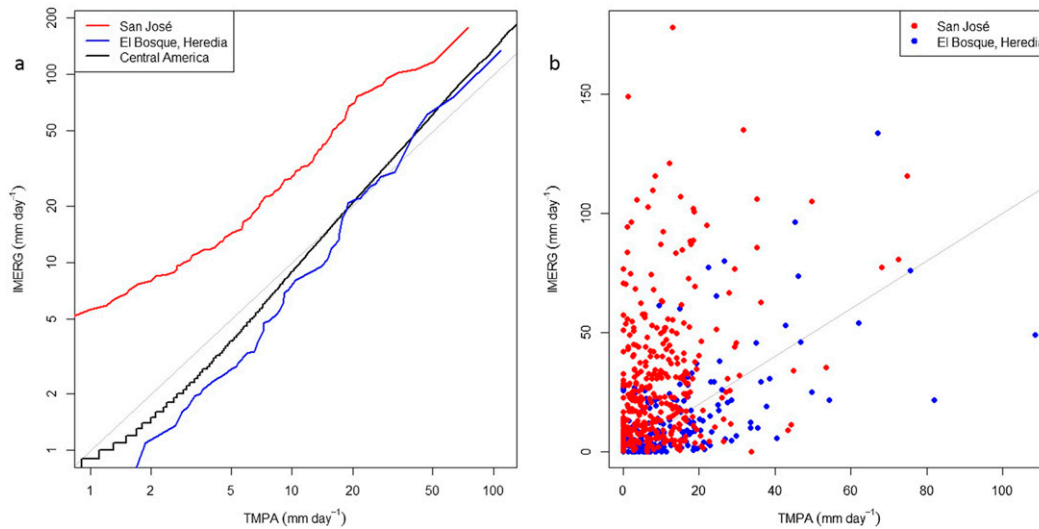


Figure 4. Quantile–quantile plot of two locations in Costa Rica as well as the whole of Central America (black). Dry days are not shown. El Bosque (blue) is separated from San José (red) by approximately 45 km, but the observed relationship between IMERG-L and TMPA-RT is dramatically different. The capital of Costa Rica has an anomalous IMERG record, in which precipitation is both heavier and more frequent.

with a high degree of spatial heterogeneity, it may be necessary to treat each pixel separately (e.g., [Wood et al. 2004](#); [Voisin et al. 2010](#)), which would require numerous data transformations and a sufficient temporal record at each point. Another approach is to calculate quantiles within a spatial sampling window ([Reichle and Koster 2004](#)). In some cases, there may be too little data that is relevant to the research topic; these studies may require a more sophisticated approach than quantile mapping.

5. Conclusions

Quantile mapping can adapt IMERG data for applications that were designed to use TMPA precipitation estimates. In Central America, a daily landslide hazard model was adapted for use with IMERG data by quantile mapping across a single domain. The results were comparable to those for the original TMPA-based model. It is likely that other long-term precipitation datasets would benefit from the same treatment. However, this method may be more successful with threshold-based models and could be impacted by low sample size at the most extreme precipitation values. Another key limitation of the method is that it must be applied over a space–time domain with a consistent relationship between TMPA and IMERG. If this requirement cannot be met, a more sophisticated treatment of the data may be required. Ultimately, a longer IMERG record will obviate the need for this technique because the user community will be able to develop new climatological datasets directly from IMERG.

Acknowledgments. This work was funded by NASA Precipitation Measurement Missions, including Proposal 15-PMM15-0038 for Dalia Kirschbaum and Thomas Stanley, 15-PMM15-0021 for George Huffman, and grant number NNX16AE20G for Robert Adler. Yudong Tian and Bin Yong provided many helpful comments. We also gratefully acknowledge the reviewers of this article for their helpful feedback.

References

- Cannon, A. J., S. R. Sobie, and T. Q. Murdock, 2015: Bias correction of GCM precipitation by quantile mapping: How well do methods preserve changes in quantiles and extremes? *J. Climate*, **28**, 6938–6959, doi:[10.1175/JCLI-D-14-00754.1](https://doi.org/10.1175/JCLI-D-14-00754.1).
- Gudmundsson, L., J. B. Bremnes, J. E. Haugen, and T. Engen Skaugen, 2012: Technical note: Downscaling RCM precipitation to the station scale using quantile mapping—A comparison of methods. *Hydrol. Earth Syst. Sci. Discuss.*, **9**, 6185–6201, doi:[10.5194/hessd-9-6185-2012](https://doi.org/10.5194/hessd-9-6185-2012).
- Hijmans, R. J., 2015: raster: Geographic data analysis and modeling. R package version 2.4-15. [Available online at <http://cran.r-project.org/package=raster>.]
- Hou, A. Y., and Coauthors, 2014: The Global Precipitation Measurement mission. *Bull. Amer. Meteor. Soc.*, **95**, 701–722, doi:[10.1175/BAMS-D-13-00164.1](https://doi.org/10.1175/BAMS-D-13-00164.1).
- Huffman, G. J., 2016a: GPM (IMERG) late precipitation L3 1 day 0.1 degree \times 0.1 degree V03. Accessed 24 May 2016. [Available online at <https://pmm.nasa.gov/data-access/downloads/gpm>.]
- , 2016b: TRMM (TMPA) real-time precipitation L3 1 day 0.1 degree \times 0.1 degree V07. Accessed 17 July 2016. [Available online at <https://pmm.nasa.gov/data-access/downloads/trmm>.]
- , and Coauthors, 2007: The TRMM Multisatellite Precipitation Analysis (TMPA): Quasi-global, multiyear, combined-sensor precipitation estimates at fine scales. *J. Hydrometeorol.*, **8**, 38–55, doi:[10.1175/JHM560.1](https://doi.org/10.1175/JHM560.1).
- , R. F. Adler, D. T. Bolvin, and E. J. Nelkin, 2010: The TRMM Multi-satellite Precipitation Analysis (TMPA). *Satellite Rainfall Applications for Surface Hydrology*, F. Hossain and M. Gebremichael, Eds., Springer Verlag, 3–22.
- , D. T. Bolvin, D. Braithwaite, K. Hsu, R. Joyce, C. Kidd, E. J. Nelkin, and P. Xie, 2015: NASA Global Precipitation Measurement (GPM) Integrated Multi-Satellite Retrievals for GPM (IMERG). Algorithm Theoretical Basis Document (ATBD) version 4.5, 30 pp. [Available online at https://pmm.nasa.gov/sites/default/files/document_files/IMERG_ATBD_V4.5_0.pdf.]
- Kirschbaum, D. B., R. F. Adler, Y. Hong, S. Hill, and A. Lerner-Lam, 2010: A global landslide catalog for hazard applications: Method, results, and limitations. *Nat. Hazards*, **52**, 561–575, doi:[10.1007/s11069-009-9401-4](https://doi.org/10.1007/s11069-009-9401-4).
- , T. Stanley, and J. Simmons, 2015a: A dynamic landslide hazard assessment system for Central America and Hispaniola. *Nat. Hazards Earth Syst. Sci.*, **15**, 2257–2272, doi:[10.5194/nhess-15-2257-2015](https://doi.org/10.5194/nhess-15-2257-2015).
- , —, and S. Yatheendradas, 2015b: Modeling landslide susceptibility over large regions with fuzzy overlay. *Landslides*, **13**, 485–496, doi:[10.1007/s10346-015-0577-2](https://doi.org/10.1007/s10346-015-0577-2).
- , —, and Y. Zhou, 2015c: Spatial and temporal analysis of a global landslide catalog. *Geomorphology*, **249**, 4–15, doi:[10.1016/j.geomorph.2015.03.016](https://doi.org/10.1016/j.geomorph.2015.03.016).
- , and Coauthors, 2017: NASA’s remotely sensed precipitation: A reservoir for applications users. *Bull. Amer. Meteor. Soc.*, doi:[10.1175/BAMS-D-15-00296.1](https://doi.org/10.1175/BAMS-D-15-00296.1), in press.
- Kucera, P. A., E. E. Ebert, F. J. Turk, V. Levizzani, D. Kirschbaum, F. J. Tapiador, A. Loew, and M. Borsche, 2013: Precipitation from space: Advancing Earth system science. *Bull. Amer. Meteor. Soc.*, **94**, 365–375, doi:[10.1175/BAMS-D-11-00171.1](https://doi.org/10.1175/BAMS-D-11-00171.1).
- Maraun, D., 2013: Bias correction, quantile mapping, and downscaling: Revisiting the inflation issue. *J. Climate*, **26**, 2137–2143, doi:[10.1175/JCLI-D-12-00821.1](https://doi.org/10.1175/JCLI-D-12-00821.1).

- Panofsky, H. A., and G. W. Brier, 1958: *Some Applications of Statistics to Meteorology*. Mineral Industries Extension Services, College of Mineral Industries, Pennsylvania State University, 224 pp. [Available online at <https://collection1.libraries.psu.edu/cdm/ref/collection/digitalbks2/id/48274>.]
- R Core Team, 2015: R: A language and environment for statistical computing. Accessed 17 July 2015. [Available online at <http://www.r-project.org/>.]
- Reichle, R. H., and R. D. Koster, 2004: Bias reduction in short records of satellite soil moisture. *Geophys. Res. Lett.*, **31**, L19501, doi:[10.1029/2004GL020938](https://doi.org/10.1029/2004GL020938).
- Turkington, T., A. Remaître, J. Ettema, H. Hussin, and C. van Westen, 2016: Assessing debris flow activity in a changing climate. *Climatic Change*, **137**, 293–305, doi:[10.1007/s10584-016-1657-6](https://doi.org/10.1007/s10584-016-1657-6).
- Voisin, N., J. C. Schaake, and D. P. Lettenmaier, 2010: Calibration and downscaling methods for quantitative ensemble precipitation forecasts. *Wea. Forecasting*, **25**, 1603–1627, doi:[10.1175/2010WAF2222367.1](https://doi.org/10.1175/2010WAF2222367.1).
- Ward, A., and D. Kirschbaum, 2014: Measuring rain for society's gain: GPM applications workshop. *Earth Obs.*, **26**, 26–34. [Available online at https://eospsso.gsfc.nasa.gov/sites/default/files/eo_pdfs/Jan-Feb_2014_final_color_508.pdf.]
- , ———, and M. Hobish, 2015: Measuring rain and snow for science and society: The Second GPM Applications Workshop. *Earth Obs.*, **27**, 4–11. [Available online at https://eospsso.gsfc.nasa.gov/sites/default/files/eo_pdfs/Sep-Oct_2015_color_508.pdf.]
- Wood, A. W., L. R. Leung, V. Sridhar, and D. P. Lettenmaier, 2004: Hydrologic implications of dynamical and statistical approaches to downscaling climate model outputs. *Climatic Change*, **62**, 189–216, doi:[10.1023/B:CLIM.0000013685.99609.9e](https://doi.org/10.1023/B:CLIM.0000013685.99609.9e).

Earth Interactions is published jointly by the American Meteorological Society, the American Geophysical Union, and the Association of American Geographers. Permission to use figures, tables, and *brief* excerpts from this journal in scientific and educational works is hereby granted provided that the source is acknowledged. Any use of material in this journal that is determined to be “fair use” under Section 107 or that satisfies the conditions specified in Section 108 of the U.S. Copyright Law (17 USC, as revised by P.L. 94-553) does not require the publishers’ permission. For permission for any other form of copying, contact one of the copublishing societies.
